frontiers in Marine Science

ORIGINAL RESEARCH
published: 24 November 2016
doi: 10.3389/fmars.2016.00232

Dark Production of Extracellular Superoxide by the Coral *Porites astreoides* and Representative Symbionts

Tong Zhang[1,2†], *Julia M. Diaz*[1,3†], *Caterina Brighi*[4], *Rachel J. Parsons*[5], *Sean McNally*[6], *Amy Apprill*[1] *and Colleen M. Hansel*[1*]

[1] Department of Marine Chemistry and Geochemistry, Woods Hole Oceanographic Institution, Woods Hole, MA, USA, [2] MOE Key Laboratory of Pollution Processes and Environmental Criteria, College of Environmental Science and Engineering, Nankai University, Tianjin, China, [3] Department of Marine Sciences, Skidaway Institute of Oceanography, University of Georgia, Savannah, GA, USA, [4] Department of Chemistry, Imperial College London, London, UK, [5] Bermuda Institute of Ocean Sciences, St. George's, Bermuda, [6] School for the Environment, University of Massachusetts Boston, Boston, MA, USA

The reactive oxygen species (ROS) superoxide has been implicated in both beneficial and detrimental processes in coral biology, ranging from pathogenic disease resistance to coral bleaching. Despite the critical role of ROS in coral health, there is a distinct lack of ROS measurements and thus an incomplete understanding of underpinning ROS sources and production mechanisms within coral systems. Here, we quantified *in situ* extracellular superoxide concentrations at the surfaces of aquaria-hosted *Porites astreoides* during a diel cycle. High concentrations of superoxide (~10's of nM) were present at coral surfaces, and these levels did not change significantly as a function of time of day. These results indicate that the coral holobiont produces extracellular superoxide in the dark, independent of photosynthesis. As a short-lived anion at physiological pH, superoxide has a limited ability to cross intact biological membranes. Further, removing surface mucus layers from the *P. astreoides* colonies did not impact external superoxide concentrations. We therefore attribute external superoxide derived from the coral holobiont under these conditions to the activity of the coral host epithelium, rather than mucus-derived epibionts or internal sources such as endosymbionts (e.g., *Symbiodinium*). However, endosymbionts likely contribute to internal ROS levels via extracellular superoxide production. Indeed, common coral symbionts, including multiple strains of *Symbiodinium* (clades A to D) and the bacterium *Endozoicomonas montiporae* LMG 24815, produced extracellular superoxide in the dark and at low light levels. Further, representative *P. astreoides* symbionts, *Symbiodinium* CCMP2456 (clade A) and *E. montiporae*, produced similar concentrations of superoxide alone and in combination with each other, in the dark and low light, and regardless of time of day. Overall, these results indicate that healthy, non-stressed *P. astreoides* and representative symbionts produce superoxide externally, which is decoupled from photosynthetic activity and circadian control. Corals may therefore produce extracellular superoxide constitutively, highlighting an unclear yet potentially beneficial role for superoxide in coral physiology and health.

Keywords: coral, superoxide, reactive oxygen species, photosynthesis, *Symbiodinium*, stress

OPEN ACCESS

Edited by:
Jörg Wiedenmann, University of Southampton, UK

Reviewed by:
Andrew Rose, Southern Cross University, Australia
Michael P. Lesser, University of New Hampshire, USA

***Correspondence:**
Colleen M. Hansel
chansel@whoi.edu

[†] *These authors have contributed equally to this work.*

Specialty section:
This article was submitted to Marine Biogeochemistry, a section of the journal Frontiers in Marine Science

Received: *12 July 2016*
Accepted: *01 November 2016*
Published: *24 November 2016*

Citation:
Zhang T, Diaz JM, Brighi C, Parsons RJ, McNally S, Apprill A and Hansel CM (2016) Dark Production of Extracellular Superoxide by the Coral Porites astreoides and Representative Symbionts. Front. Mar. Sci. 3:232. doi: 10.3389/fmars.2016.00232

INTRODUCTION

Cellular redox homeostasis is required for the proper biological functioning and health of all living systems. Reactive oxygen species (ROS)—including the superoxide anion ($O_2^{\bullet-}$), its conjugate acid the hydroperoxyl radical ($HO_2^{\bullet}$), hydrogen peroxide (H_2O_2), and the hydroxyl radical ($HO^{\bullet}$)—can threaten this homeostasis, based on their ability to degrade vital cell components such as lipids and DNA (Lesser, 2006), as well as their capacity to activate programmed cell death pathways (Cai and Jones, 1998). ROS are an inevitable consequence of aerobic life and commonly arise as metabolic byproducts in oxygenated cells. In contrast to such hazardous intracellular ROS production, however, recent evidence highlights the benefits of extracellular ROS to the physiological health and functioning of macro- and micro-organisms, including bacteria (Saran, 2003; Buetler et al., 2004), fungi (Aguirre et al., 2005), algae (Kustka et al., 2005; Rose et al., 2005, 2008b; Weinberger, 2007; Roe and Barbeau, 2014), plants (Minibayeva et al., 2009), and animals (Babior, 1999). For instance, ROS can serve in autocrine growth (Oda et al., 1995; Saran, 2003; Buetler et al., 2004), immune defense (Babior, 1999; Weinberger, 2007), metal nutrient acquisition (Rose et al., 2005; Fujii et al., 2010; Roe and Barbeau, 2014), wound repair (Minibayeva et al., 2009), and cell differentiation (Aguirre et al., 2005).

In corals, intracellular ROS production, typically stimulated by excessive heat exposure, has a negative role in coral health by causing oxidative stress and bleaching, or the loss of essential photosynthetic endosymbiotic *Symbiodinium* algae (Lesser, 2011). The key source of intracellular ROS in stressed corals is thought to be disrupted photosynthetic electron transport in *Symbiodinium* and the coral mitochondria, which leads to the reduction of endogenous photosynthetically-derived O_2 (Jones et al., 1998; Tchernov et al., 2004; Lesser, 2006; Venn et al., 2008; Weis, 2008). In contrast, corals also produce ROS externally (Saragosti et al., 2010; Shaked and Armoza-Zvuloni, 2013), which involves the reduction of exogenous O_2 in seawater at the coral surface. Extracellular and intracellular ROS production therefore occurs via independent pathways in corals, as depicted in **Figure 1**. Specifically, photosynthetic superoxide production should not contribute directly to external superoxide concentrations (**Figure 1**). Photosynthetically derived intracellular ROS in corals occurs within *Symbiodinium*, which localize in membrane-bound symbiosomes inside the coral host's inner gastrodermal cell layer. Despite the ability of hydroperoxyl radical (the protonated form of superoxide, $HO_2^{\bullet}$) to diffuse through membranes at a rate approaching that of water, superoxide anion ($O_2^{\bullet-}$) dominates in pH conditions above 4.8 (Bielski et al., 1985) and has a limited ability to diffuse across membranes (Korshunov and Imlay, 2002). Recent evidence that the symbiosome has a pH of ∼4 (Barott et al., 2015) may indicate that superoxide could diffuse from the symbiosome into the gastrodermal coral cells. Yet, unprotonated superoxide would dominate once in coral gastrodermal cells, which have a pH of ∼7 (Venn et al., 2009; Barott et al., 2015). Thus, as an anion at the physiological pH conditions within the coral tissues, superoxide is likely incapable of crossing the many biological membranes that separate the photosynthetic electron transport chain of *Symbiodinium* from seawater (Rose, 2012) (see **Figure 1**). In addition, the typical intracellular lifetime (∼ μs) and diffusive distance of superoxide (∼100′s of nm) (Lesser, 2006) are also too short to allow extensive transport from its site of production within *Symbiodinium*.

Instead, extracellular superoxide production by corals likely originates from the coral host's epithelial cells or epibionts, including bacteria within the coral mucus layer (**Figure 1**). This external superoxide production probably occurs through the activity of extracellular oxidoreductase enzymes, such as NAD(P)H oxidases (Babior, 1999; Saran, 2003; Aguirre et al., 2005; Kustka et al., 2005; Rose et al., 2005; Weinberger, 2007; Andeer et al., 2015). Indeed, the inhibition of coral-derived extracellular superoxide production by the broad spectrum NADPH oxidoreductase inhibitor diphenyleneiodonium (DPI) suggested that extracellular superoxide production by corals is mediated by this large and diverse family of NAD(P)H-oxidizing enzymes (Saragosti et al., 2010), similar to other organisms, such as mammalian leukocytes (Babior, 1999), fungi (Aguirre et al., 2005), macroalgae (Weinberger, 2007), phytoplankton (Kustka et al., 2005; Rose et al., 2005), bacteria (Andeer et al., 2015), and plants (Minibayeva et al., 2009). Photosynthesis may play an indirect role in the production of external superoxide by corals by supplying NADPH that stimulates the activity of superoxide-producing oxidoreductases on the coral surface (Saragosti et al., 2010). This indirect involvement of photosynthesis in extracellular superoxide generation may also explain previous observations of light-stimulated extracellular superoxide production by phytoplankton, including the colonial diazotroph *Trichodesmium* (Hansel et al., 2016) and *Symbiodinium* (Saragosti et al., 2010), which also likely generate extracellular superoxide via cell surface associated NAD(P)H oxidoreductases.

In addition to their production through independent physiological pathways, intra- and extracellular superoxide may also have fundamentally different physiological consequences to coral health. For instance, dark production of extracellular superoxide has been observed in unstressed corals (Saragosti et al., 2010), *Symbiodinium* (Saragosti et al., 2010), and bacterial genera commonly associated with corals (Diaz et al., 2013), suggesting a constitutive role for external superoxide in healthy biological systems. Although the underlying reasons for this production remain unresolved, recent observations suggest that external ROS production, and NADPH oxidoreductases putatively involved in superoxide production, may promote coral thermotolerance (Dixon et al., 2015), immune defense (Banin et al., 2003; Libro et al., 2013), and prey acquisition (Armoza-Zvuloni et al., 2016).

The goal of the current study was to investigate the dark production of external superoxide by unstressed corals and cultured representatives of their microbial symbionts. While direct measurements of ROS within coral tissues are difficult and artifact-prone, recent advances in chemiluminescent techniques have made non-invasive measurements of external superoxide production by corals and their symbionts more tractable. Here, we measured external superoxide production

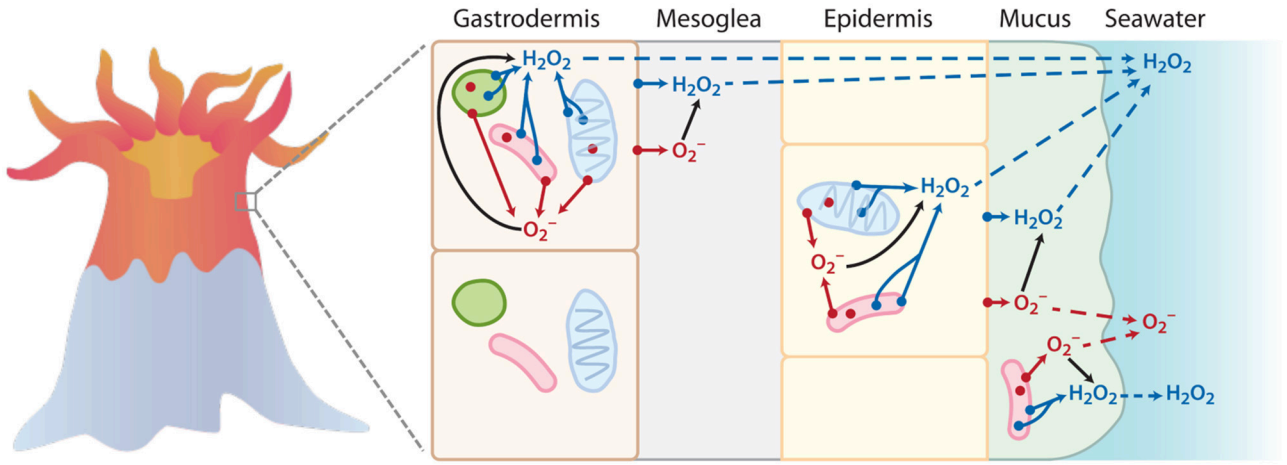

FIGURE 1 | Simplified schematic to illustrate the points of origin (denoted by a dot) for superoxide (O_2^-) (in red) and hydrogen peroxide (H_2O_2) (in blue) within coral tissue. The outer membranes of host cells, mitochondria (blue oval), *Symbiodinium* (green circle), and bacteria (pink rod) are represented as potential sites of intracellular and extracellular ROS production (not to scale). While this schematic may not depict all the possible sources of superoxide and hydrogen peroxide production in corals, it is meant to provide a simple conceptual framework. In particular, the superoxide anion only has a limited ability to cross membranes at physiological pH, and thus intracellular formation of superoxide does not significantly impact extracellular pools. In contrast, hydrogen peroxide can travel throughout the coral tissue (transport denoted by dotted lines), and thus intracellular hydrogen peroxide sources can contribute to extracellular pools. Superoxide produced outside of cells via extracellular or transmembrane proteins can interact with surrounding cells. For instance, extracellular superoxide production by *Symbiodinium* or bacteria could directly interact with coral cells (see top gastrodermal cell). Direct measurements of external superoxide would likely include superoxide formed at the plasma membrane of coral epithelial cells as well as extracellular superoxide generated by bacteria in the mucus layer.

from aquaria-hosted *Porites astreoides* corals in the dark and low light levels at two times during the day. *P. astreoides* was chosen as a representative coral because it is found in a variety of reef habitats around the world and has been associated with Caribbean reefs for millennia (Pandolfi and Jackson, 2006). The high recruitment success of *P. astreoides* has helped to increase the relative abundance of this species on Caribbean reefs (Green et al., 2008) and its microbial community has been well-described (Rohwer et al., 2002; Morrow et al., 2012; Rodriguez-Lanetty et al., 2013). In addition to *P. astreoides*, we identified and then examined representative cultures of its microbial symbionts for the ability to produce extracellular superoxide within corals. As coral-*Symbiodinium* relationships can be flexible, we further examined the ability of diverse *Symbiodinium* clades to produce extracellular superoxide.

MATERIALS AND METHODS

Coral Collection and Aquaria Incubations

Porites astreoides colonies were collected from 3–9 m water depth at 3 sites in Bermuda in July 2013: Hog Breaker Reef (N 32° 27.5′ W 64° 49.8′), an unnamed patch reef (N 32° 26.042′ W 64° 49.248′), and Three Hill Shoals (N 32° 41′ W 64° 73.3′). The mid-day photosynthetically active radiation (PAR) at coral depth in these reefs was ∼300–500 μmol photon m^{-2} s^{-1}. Colonies ranged from 15–20 cm diameter, and colonies of similar size were specifically selected to avoid the need for surface area normalization of superoxide measurements. *P. astreoides* colonies were placed in collection bags, which were sealed underwater. Upon surfacing, the corals were transferred into a cooler containing reef water from the site and transported (<1 h) to the laboratory at the Bermuda Institute of Ocean Sciences (BIOS). Ten colonies were taken from each site ($n = 30$) in compliance with the BIOS Collection and Experimental Ethics Policy (CEEP). This was considered Limited Impact Research, and as such a collection permit was not required.

At BIOS, specimens were placed in outdoor fiberglass holding aquaria for 2 days to allow them to acclimate to *ex situ* conditions. Following acclimation in the holding aquaria, *P. astreoides* colonies were transferred to indoor aquaria outfitted with a lighting system configured with full spectrum LED lamps and a light controller that simulates a daily light cycle (PAR = ∼100 μmol photon m^{-2} s^{-1}). PAR at the surface of the corals in the tanks was 61 μmol photon m^{-2} s^{-1}, which is lower than the mid-day light conditions on the reef (see above). While these levels are low, they are in the range of known compensation ranges for photosynthetic activity [3–233 μmol photon m^{-2} s^{-1}, (Mass et al., 2007)]; yet, where *P. astreoides* falls within this range is currently unknown, and thus the level of photosynthesis occurring under the low light conditions used for this study is unknown. Three coral colonies were placed in each of three replicate aquaria and acclimated for an additional 2 days before starting superoxide measurements. Control aquaria, in which corals were absent, were incubated under the same conditions. Each aquarium was fed with local seawater from Ferry Reach. Briefly, water from 20 m off shore and one meter in depth was pumped through a BIOS flow-through sample system that consisted of a coarse mesh filter followed by a step filtration system of 50 μm, then 5 μm, to remove larger organisms including

some planktonic grazers. The flow-through system was equipped with air wand bubblers to provide constant aeration and mixing.

For a subset of corals, mucus was removed from the coral surfaces by inverting coral heads for 2 h, which was previously determined to be the optimal time for removing the majority of surface mucus layer while not compromising coral health.

Extracellular Superoxide Measurements of Aquaria-Hosted Corals

Superoxide concentrations were measured with a flow-through FeLume Mini system (Waterville Analytical, Waterville ME) via the specific reaction between superoxide and the chemiluminescent probe methyl *Cypridina* luciferin analog (MCLA, Santa Cruz Biotechnology). The FeLume system is composed of two separate fluid lines, one of which is dedicated to the analyte solution and the other to the MCLA reagent. The reagent was amended with 100 μM diethylene-triaminepentaacetic acid (DTPA) in order to sequester trace metal contaminants that would otherwise significantly reduce the lifetime of superoxide. To measure superoxide, both the analyte solution and the MCLA reagent were independently flushed through the FeLume system at an identical flow rate (i.e., 2 mL min^{-1}) using a peristaltic pump. The solutions converge in a spiral flow cell immediately adjacent to a photomultiplier tube, which continuously acquires data that is displayed in real time using a PC interface. The MCLA reagent consisted of 4.0 μM MCLA with 100 μM DTPA in 0.10 M MES buffer adjusted to pH 6.0. In previous studies, concentrations of the MCLA reagent ranged from 1 to 5 μM (Rose et al., 2008a, 2010; Heller and Croot, 2010; Roe et al., 2016; Zhang et al., 2016), depending on the sensitivity required.

For measurements of superoxide in aquaria, a cart adjacent to the aquaria was used to host the FeLume in order to reduce the length of tubing (travel time) required to transport the water from the aquaria to the instrument. To eliminate abiotic photochemical processes that may produce superoxide during *in situ* measurements, opaque tubing was used, and the entire analytical system was shielded from light. Seawater was directly pumped into the FeLume by placing the analyte tubing at discrete positions within the aquarium in relation to the corals. For each aquarium, a number of superoxide measurements were conducted. First, a baseline was acquired from a reagent blank to account for the chemiluminescence signal resulting from the autooxidation of MCLA. The reagent blank consisted of aged filtered seawater (AFSW) amended with DTPA (AFSW+DTPA). To prepare AFSW+DTPA, Ferry Reach water was collected from the flow-through system and filtered (0.2-μm Sterivex™, Millipore). The filtered seawater was aged in the dark (>12 h) to deplete superoxide, amended with 50 μM DTPA, and left in the dark for an additional 12 h to allow DTPA to complex trace metals.

After running the reagent blank, the seawater signal was measured at two background locations in the aquarium: First, a position in the water at the top of the tank and second, at the same depth as the corals but 2–3 cm away (horizontal distance). Data were acquired until a stable, steady-state reading was achieved (< ∼4% coefficient of variation). The tubing was then moved to the seawater immediately adjacent to the coral (<1 cm away from the coral, without touching the surface of the coral). Seven measurements were made at various locations along the coral surfaces. The tubing was then moved back to the background seawater at positions that were equivalent to the initial background measurements. Data were acquired for at least 2 min to ensure that the signals returned to the original background values. Finally, superoxide dismutase (SOD), an enzyme that rapidly degrades superoxide, was added (800 U L^{-1} SOD) to an aliquot of water taken from the coral surface in order to confirm that the signal was in fact attributable to superoxide. SOD routinely lowers the signal derived from the reagent blank, likely reflecting a small concentration of superoxide present in the AFSW+DTPA or more likely produced during the auto-oxidation of MCLA (Hansard et al., 2010).

Before converting superoxide chemiluminescence signals to concentrations, all measurements were corrected by subtracting the signal obtained from the reagent blank. Superoxide concentrations were not corrected for decay that occurred within the tubing during the brief time required to pump the sample from the point in the aquaria into the FeLume, and thus the values represent conservative estimates. Chemiluminescence signals were calibrated by generating stock solutions of superoxide from potassium dioxide (KO_2). Considering the short lifetime of superoxide, standards were prepared immediately before analysis. Primary stock solutions were made by dissolving a small quantity of KO_2 in a basic matrix (0.03 N NaOH, 50–100 μM DTPA, pH = 12.5). Superoxide concentrations in primary standards were quantified by measuring the difference in absorbance at 240 nm before and after the addition of SOD (∼8 U mL^{-1}, final) and then converting to molar units based on the molar absorptivity of superoxide (2183 L mol^{-1} cm^{-1} at 240 nm, pH = 12.5, and corrected for the absorption of hydrogen peroxide formed during decay) (Bielski et al., 1985). Primary stocks had to be substantially diluted in order to generate representative concentrations for analysis on the FeLume. To generate secondary stocks (4–55 nM), the primary stock solution was diluted into AFSW+DTPA. For each calibration point, a separate FeLume run was conducted as follows: First, the reagent blank was run until a stable baseline (<4% coefficient of variation) was achieved for ∼1 min. Then the secondary standards were pumped directly into the FeLume, and the decay of superoxide was monitored for at least 1 min. Finally, SOD was added to the secondary standard (∼0.8 U mL^{-1}, final) in order to confirm that the signal was attributable to superoxide.

Chemiluminescence signals collected during the decay of superoxide standards were extrapolated backwards in time to the point when the primary standard was quantified spectrophotometrically. Extrapolations assumed first order decay kinetics because decay data were log-linear. Multi-point calibration curves were constructed based on the linear regression of several pairs of extrapolated luminescence signals vs. superoxide concentrations. Calibrations yielded linear curves (e.g., $R^2 > 0.94$), with a sensitivity that ranged from 0.09 to 0.11 luminescence units per pM superoxide. The half-life of

superoxide in the calibration matrices ranged from 0.89 to 2.11 min and the extrapolation time was 0.93–1.27 min. The detection limit of this method, calculated as three times the standard deviation of a series of blank measurements, was 0.13 nM. Superoxide measurements were compared using unpaired two-sample *t*-tests.

Ancillary Data from Aquaria Water

Water temperature, pH, salinity and dissolved oxygen (DO), were measured using a YSI 556MPS handheld multiparameter system. The YSI pH probe consists of a glass bulb filled with a stable pH = 7 reference solution. The potential across the glass surface created between the water sample and reference solution is measured and converted to pH using a 3-point calibration (pH 4, 7, 10). For the analysis of metals, including total dissolved iron (Fe), manganese (Mn), and copper (Cu), triplicate samples were taken from aquaria surface water on days 1, 4, and 7. Samples were filtered (0.2-μm), amended with 2% (v/v) nitric acid (HNO_3, trace metal grade), and analyzed using inductively coupled plasma mass spectroscopy (ICP-MS).

Identification of *P. astreoides* Symbionts

Bacteria, archaea, and *Symbiodinium* were identified from tissue and mucus homogenates from six *P. astreoides* colonies and mucus from 10–12 colonies. Samples for symbiont identification were taken after all superoxide measurements. Tissue was frozen (−80°C), airbrushed, and extracted using the Power Plant DNA extraction kit (Mo Bio laboratories), using a modified protocol described previously (Apprill et al., 2013). Briefly, the modifications to the extraction protocol included two enzyme digestions including a 10 units/μL addition of lysozyme (Ready-Lyse Lysozyme Solution, #R1802M) for 10 min at room temperature and an addition of 20 mg/mL of proteinase K (Qiagen) incubated at 65°C for 10 min at 1000 RPM. Processing of mucus samples followed a method modified from Giovannoni et al. (1990, 1996). Briefly, mucus (1 mL) was filtered (0.2 μm) under gentle vacuum (∼100 mm Hg), and stored in lysis buffer (20 mM EDTA, 400 mM NaCl, 0.75 M sucrose, 50 mM Tris.HCl) at −80°C. For DNA extraction, sodium dodecyl sulfate (1% final) and proteinase K (200 μg mL^{-1} final) were added to the sample and incubated at 37 °C for 30 min and then at 55°C for 30 min. The lysates were extracted with an equal volume of phenol:isoamylalcohol:chloroform (25:1:24) followed by two subsequent equal volumes of isoamylalcohol:chloroform (1:24). Purification of the DNA was conducted using sodium acetate (3 M) and isopropanol for at least 1 h at −20° C and centrifuged (20,000 × g) at room temperature for 30 min. The resulting pellet was washed with 80% ethanol, vortexed for 30 s and centrifuged at 16,000 × g for 10 min.

Bacterial and archaeal community composition was assessed by targeting the V4 region of the SSU rRNA gene using modified primers, 515F and 806RB (Apprill et al., 2015). Triplicate 25 μL PCR reactions were conducted per sample, which consisted of 1.25 U GoTaq Flexi DNA Polymerase (Promega), 5X Colorless GoTaq Flexi Buffer, 2.5 mM $MgCl_2$, 200 μM dNTP mix, 200 nM of each barcoded primer, and 1–4 ng of genomic template. The reactions were carried out on a thermocycler (Bio-Rad Laboratories) with the following conditions: An initial denaturation step at 95°C for 2 min; 27–32 cycles of 95°C for 20 s, 55°C for 15 s, and 72°C for 5 min; concluding with an extension at 72°C for 10 min. Reaction products (5 μL) were screened on a 1% agarose/TBE gel using a HyperLadder 50 bp standard (generally 5 ng μL^{-1}) (Bioline). Replicate reactions were purified using the QIAquick Purification Kit (Qiagen), and quantified using the Qubit fluorescent broad range dsDNA assay (Life Technologies). Amplicons were pooled in equimolar ratios and shipped to the University of Illinois W.M. Keck Center for Comparative and Functional Genomics for preparation and sequencing using 250 bp paired-end MiSeq (Illumina), as detailed previously (Kozich et al., 2013). Sequence analyses were conducted using mothur v.3.3.3 (Schloss et al., 2009) and included assembly of the paired ends, amplicon size selection (253 bp median size) and alignment to the SSU rRNA gene. Chimera detection was also conducted via UCHIME (Edgar et al., 2011) in mothur, and chimeric sequences were subsequently removed. Taxonomic classification of sequences was conducted using the k-nearest neighbor algorithm with the SILVA SSU Ref database (release 119). Sequence data are available at NCBI's SRA under accession PRJNA 312300.

Symbiodinium taxonomy was resolved using a portion of the chloroplast 23S rRNA gene using primers 23S1 (5′-GGCTGTAACTATAACGGTCC-3′) and 23S2 (5′-CCATCGTA TTGAACCCAGC-3′) (Zhang et al., 2000). Each sample was amplified in triplicate reactions with 1.25 U of GoTaq Flexi DNA Polymerase, 5X Colorless GoTaq Flexi Buffer, 2.5 mM $MgCl_2$, 200 μM dNTP mix, 200 nM of each barcoded primer, and 4–9 ng of genomic template. The reactions were carried out on a Bio-Rad thermocycler with the following conditions: 95°C for 7 min followed by 39 cycles of 95°C for 45 s, 55°C for 45 s, and 72°C for 45 s. An additional extension step that was made at 72°C for 10 min concluded the reaction. Reaction products were visualized, gel excised and purified using the QIAquick gel extraction kit (Qiagen). Purified products were cloned (32 clones per colony) using the pGem-T Easy system (Promega) and shipped to Beckman Coulter Genomics for single pass Sanger sequencing. Clade affiliation was determined by aligning to reference sequences previously identified by Pochon and colleagues (Pochon et al., 2012) using ClustalW and visualizing with a weighted guide tree all within MacVector (v. 14.5.3, Apex). Sequence data are available at NCBI under accessions KX885228-KX885405.

Symbiont Cultures

Endozoicomonas montiporae LMG24815 and a member of *Symbiodinium* clade A4, *Symbiodinium* CCMP2456, were chosen as representative *P. astreoides* symbionts. *E. montiporae* LMG 24815, which was originally isolated from the coral *Montipora aequituberculata* (Yang et al., 2010) was obtained from the Belgian Co-ordinated Collections of Micro-organisms culture repositories. *E. montiporae* was grown in liquid marine broth at 23°C, and growth was quantified with cell counts after staining with 2-(4-amidinophenyl)-1H-indole-6-carboxamidine (DAPI) (Porter and Feig, 1980). *Symbiodinium* cultures (CCMP2456, CCMP2470, CCMP3364, CCMP2466,

CCMP3408, and CCMP2556) were obtained from the National Center for Marine Algae and Microbiota (NCMA, and formerly the CCMP), Bigelow Laboratories, East Boothbay, ME. *Symbiodinium* cultures were grown in L1 media (Guillard and Hargraves, 1993) using filtered (0.2 μm) natural seawater (Vineyard Sound, MA) as a base. All *Symbiodinium* cultures were incubated at 23°C using 140 μmol photons m^{-2} s^{-1} on a 14:10 h light:dark cycle, and growth was tracked by monitoring the relative fluorescence of chlorophyll with a Turner fluorometer (AquaFluor®). *Symbiodinium* cell counts were performed under transmitted light using a counting chamber, following preservation with Lugol's solution (2%, final concentration).

Extracellular Superoxide Production by Symbiont Cultures

The ability of coral symbionts to produce extracellular superoxide in the dark and in the presence of ambient light (PAR = 45–60 μmol photon m^{-2} s^{-1}) was examined during the day (∼9am–1pm) and, in select cases, at night (∼8–11pm). These ambient light levels were likely, though not confirmed, near the compensation point (Savage et al., 2002) for photosynthesis, particularly since the *Symbiodinium* light microenvironment *in hospite* is greatly reduced compared to surface irradiance levels (Lichtenberg et al., 2016). Representative *P. astreoides* symbionts (*Symbiodinium* CCMP2456 and *E. montiporae*) were screened for extracellular superoxide production separately and together in a full-factorial day/night, low light/dark experiment. For experiments involving the combination of *Symbiodinium* CCMP2456 and *E. montiporae*, cultures were mixed immediately prior to analysis. In low light experiments, ambient PAR originated mainly from the laboratory lights and natural sunlight through the lab windows. For experiments conducted in the dark, lab lights were switched off, and the entire FeLume system was shielded from light using a professional-grade dark bag designed for changing photography film. In all experiments, opaque tubing was utilized in order to eliminate abiotic photo-production of superoxide in the sample tubing.

Extracellular superoxide produced by laboratory cultures was measured using a previously described MCLA/FeLume method (Diaz et al., 2013) with a few modifications (see above for general description of the FeLume system). Briefly, carrier solutions consisting of artificial seawater (Van Waasbergen et al., 1993) buffered with 20 mM phosphate (pH = 7.6) and amended with DTPA (75 μM) were gently pumped (2 mL min^{-1}) across a sterile syringe filter placed in the FeLume's analyte line for approximately 2 min in order to generate stable baseline signals (<4% coefficient of variation). Next, the pump was stopped, the syringe filter was removed, and using a syringe, organisms were gently deposited on the filter (*Symbiodinium* = 0.2 or 5 μm, *E. montiporae* = 0.2 μm, *Symbiodinium* + *E. montiporae* = 0.2 μm). Then the organism-loaded filter was placed back inline, and the pump was restarted (2 mL min^{-1}). In principle, superoxide produced extracellularly is entrained by the carrier solution and detected upon mixing with MCLA in the flow cell downstream of the organisms. Biological signals were collected until a stable, steady-state reading was achieved (< ∼4% coefficient of variation) and maintained for at least 1 min. Finally, SOD was added to the carrier solution (0.8 U mL^{-1}, final) in order to confirm that superoxide was responsible for the signal observed.

Stable biological signals were averaged and corrected for background luminescence by subtracting the average initial baseline (i.e., obtained with the clean syringe filter inline, immediately before the addition of organisms and without the addition of SOD). Corrected biological signals were converted to superoxide concentrations via calibration with multi-point KO_2 standard curves under identical conditions as biological experiments, similar to the protocol described elsewhere (Diaz et al., 2013) and outlined above for the aquaria superoxide measurements. The typical detection limit [defined as three times the average standard deviation (*SD*) of replicate baseline signals] was 0.24 ± 0.11 nM (avg ± *SD*). As determined from calibration experiments, superoxide half-lives varied inversely with superoxide concentration and ranged from 1.1–38.5 min, and extrapolation times were typically 64.6 ± 10.6 s (avg ± *SD*) under our experimental conditions. Biogenic superoxide concentrations were not corrected for superoxide decay and thus represent conservative estimates. As above, calibrations yielded linear curves (e.g., $R^2 > 0.92$), with a sensitivity that averaged 2.2 ± 0.6 pM per luminescence count.

Net superoxide production rates were calculated as the product of the steady-state superoxide concentration and flow rate (final units of pmol h^{-1}). The production rate of superoxide by each replicate was normalized to the total number of cells loaded on the filter (final units of amol $cell^{-1}$ h^{-1}). Cell normalized production rates were converted to surface-area normalized rates (amol μm^{-2} h^{-1}). Surface area (*SA*) for each organism was calculated based on its typical length (*l*) and width (*w*). For *Symbiodinium, SA* was calculated as a sphere, $S = 4\pi r^2$, where $r = \frac{l}{2} = \frac{w}{2}$; or prolate spheroid $SA = 2\pi B^2 \left(1 + \frac{A\sin^{-1}(m))}{mB}\right)$, where $A = \frac{l}{2}, B = \frac{w}{2}$ and $m = \sqrt{1 - (\frac{B}{A})^2}$. For *E. montiporae*, SA was calculated as a rod ($SA = 4\pi s^2 + 2\pi sl$), where $s = \frac{w}{2}$. Superoxide measurements were compared using unpaired two-sample *t*-tests.

RESULTS

P. astreoides Aquaria Incubations

Physiochemical measurements confirmed that corals had acclimated to indoor aquaria conditions within 2 days, based on similar temperature, pH, dissolved oxygen, conductivity, and salinity between control and coral-containing tanks (**Table 1**). The concentrations of dissolved Fe, Mn, and Cu in control aquaria were consistently higher than those in coral aquaria, and the metal concentrations decreased with time in all aquaria (**Table 2**).

Superoxide was measured on days 3–7 following the placement of corals in the indoor aquaria, During these days, superoxide in surface seawater from the three control aquaria (no corals) ranged from 0.5 to 4.4 nM (**Figure 2**), with an

TABLE 1 | Geochemical measurements in tanks.*

	Day#							
	0	1	2	3	4	5	6	7
CONTROL TANKS								
Temperature (°C)	26.3 (0.3)	24.1 (0.2)	24.0 (0.2)	24.3 (0.2)	24.2 (0.1)	24.6 (0.3)	24.9 (0.2)	24.5 (0.0)
Dissolved Oxygen (%)	104 (1)	104 (1)	104 (1)	104 (2)	104 (1)	104 (2)	108 (1)	105 (0)
Conductivity (mS/cm)	55.3 (0.1)	56.1 (0.1)	56.7 (0.4)	57.1 (0.5)	57.7 (0.6)	58.1 (0.6)	57.4 (0.6)	58.2 (0.7)
Salinity (PSU)	36.7 (0.0)	37.3 (0.1)	37.7 (0.4)	38.1 (0.5)	38.5 (0.5)	38.8 (0.5)	38.2 (0.4)	39.0 (0.6)
pH	8.04 (0.02)	8.08 (0.01)	8.08 (0.02)	8.12 (0.02)	8.16 (0.02)	8.20 (0.01)	8.21 (0.01)	8.14 (0.02)
CORAL TANKS								
Temperature (°C)	26.2 (0.2)	24.1 (0.2)	24.1 (0.2)	24.3 (0.0)	24.2 (0.1)	24.6 (0.2)	24.8 (0.2)	24.5 (0.0)
Dissolved Oxygen (%)	104 (1)	104 (3)	102 (1)	104 (3)	103 (1)	104 (0)	108 (0)	104 (2)
Conductivity (mS/cm)	55.4 (0.1)	56.3 (0.3)	57.0 (0.5)	57.6 (0.5)	58.1 (0.5)	58.7 (0.5)	57.5 (0.4)	58.7 (0.4)
Salinity (PSU)	36.7 (0.0)	37.1 (0.4)	38.0 (0.4)	38.4 (0.4)	38.8 (0.4)	39.2 (0.3)	38.3 (0.3)	39.2 (0.4)
pH	8.03 (0.02)	8.03 (0.03)	8.04 (0.02)	8.07 (0.01)	8.10 (0.01)	8.14 (0.00)	8.13 (0.01)	8.04 (0.02)

Mean value for three replicate tanks; standard deviation in parentheses.
#*Superoxide measurements made on days 3 through 7.*

TABLE 2 | Metal concentrations# in aquaria water.

Tank	Day	Fe (mg/L)	Mn (mg/L)	Cu (mg/L)
Control	1	141.0 ± 20.1	2.3 ± 0.4	38.1 ± 4.4
	4	170.0 ± 97.4	1.0 ± 0.3	25.1 ± 2.3
	7	56.9 ± 14.4	0.7 ± 0.2	21.7 ± 2.5
Coral	1	58.0 ± 16.6	0.8 ± 0.1	23.1 ± 3.6
	4	47.1 ± 8.2	0.7 ± 0.1	17.1 ± 6.8
	7	31.6 ± 9.7	0.4 ± 0.0	17.6 ± 2.0

#*Values represent mean ± standard deviation of triplicate samples.*

average value of 2.3 ± 1.1 nM (mean ± *SD*, $n = 30$). These concentrations did not change significantly throughout the day. For example, in the morning (9 am) with low lights on, the average superoxide concentration in control seawater was 2.3 ± 0.9 nM. In the dark at night (9 pm), the average superoxide concentration was 2.2 ± 1.2 nM, which was statistically similar to morning concentrations ($p = 0.8$). Only on day 4 was a significant ($p < 0.05$) difference observed between morning and night superoxide concentrations within the control aquaria.

The concentration of superoxide at the top of coral-containing aquaria ranged from 0.1 to 1.4 nM. These superoxide concentrations were typically lower (average 0.6 ± 0.3 nM; $n = 30$) than those observed in the control aquaria without corals (average 2.3 ± 1.1 nM), but this difference was only significant ($p < 0.05$) on days 4 (am and pm), 5 (am and pm), and 7 (am only) (**Figure 2**). The superoxide concentration in the seawater approximately 3 cm from the corals ranged from 0.2 to 1.7 nM, with an average value of 0.9 ± 0.4 nM. These concentrations were not significantly different than the surface water measurements, except for two time points (day 4 and day 7 at 9 pm) when the concentrations were significantly ($p < 0.05$) higher. Similar to control aquaria without corals, background superoxide concentrations in coral-containing aquaria were similar from day to night ($p > 0.05$).

Superoxide concentrations directly at the surface of the corals were significantly ($p < 0.05$) higher than superoxide measured in control aquaria and at background locations within the coral-containing aquaria. The average superoxide concentration at coral surfaces was 35.0 ± 8.1 nM ($n = 30$), and the range of superoxide concentrations at coral surfaces was 21.3 to 50.3 nM (**Figure 2**). Coral-derived superoxide concentrations did not vary significantly over the 5-day incubation period. Although average superoxide concentrations at coral surfaces were higher in the morning in the presence of low light compared to the dark night values, these differences were only significant for one time point (day 5). Even for this time point, however, dark production accounted for 79% of the superoxide produced in the presence of low light in the morning.

For one aquarium incubation, mucus was removed from the coral surface and the corals were placed back in the aquarium. Superoxide measurements on these low-mucus corals were made within an hour. The tank-surface water and water 3 cm from the coral surface were 0.2 nM ($n = 1$) and 0.5 ± 0.1 nM ($n = 2$), respectively. The average concentration of superoxide at the coral surface was 47.7 ± 12.3 nM ($n = 7$), which was not significantly different than corals that did not undergo mucus removal (**Figure 2**).

Identification of *P. astreoides* Symbionts

Cloning and sequencing of chloroplast 23S rRNA genes demonstrated that the experimental corals all contained *Symbiodinium* belonging to clade A (32 clones each from 6 colonies). In both the mucus and the combined mucus and tissue samples, bacterial and archaeal SSU rRNA gene sequencing revealed that communities were dominated by sequences affiliated with the *Endozoicomonas* genus of Gammaproteobacteria (*Oceanospirillales* family) (**Table 3**). Relative abundances of *Endozoicomonas* sequences were higher

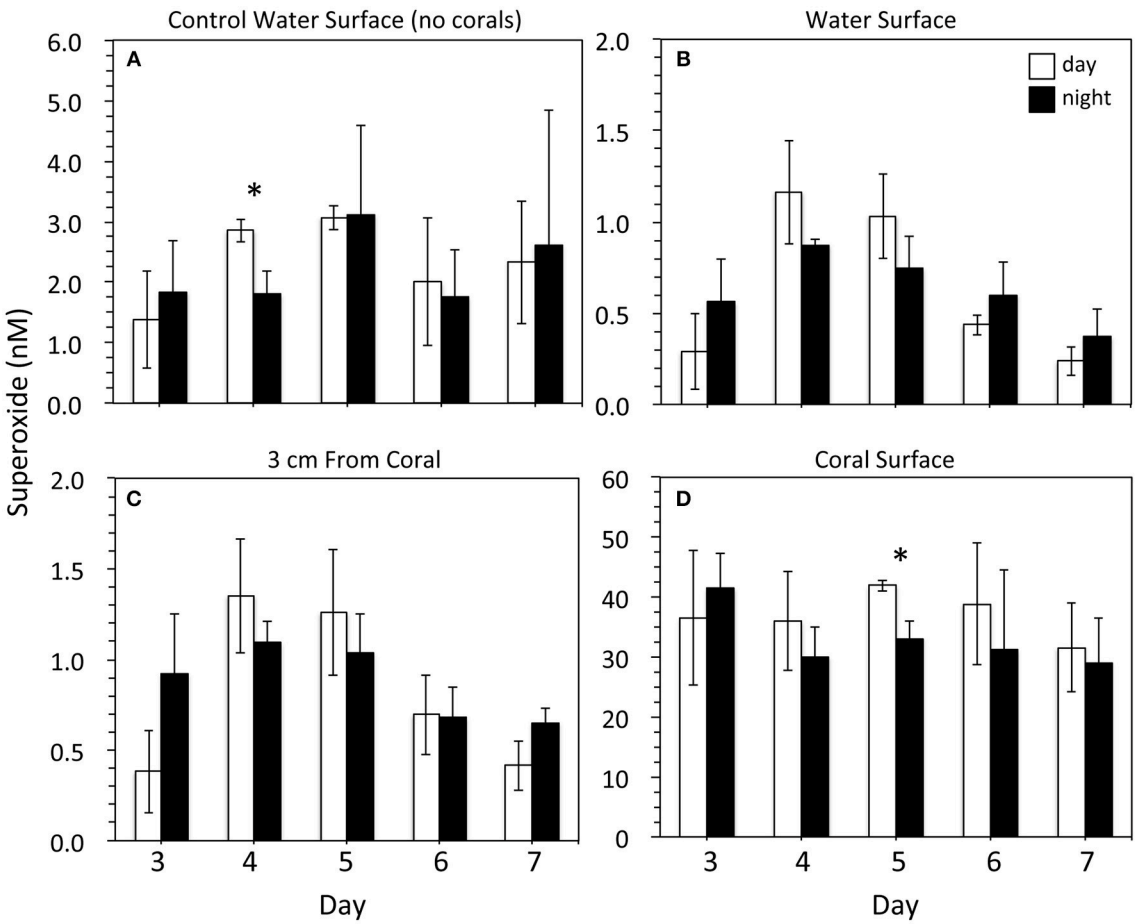

FIGURE 2 | Superoxide concentrations within (A) control tanks containing just seawater ($n = 3$) and **(B–D)** tanks containing three *Porites astreoides* colonies ($n = 3$). For each coral tank, measurements were taken at one position in the surface water (**B**; $n = 3$), 2 positions ~3 cm away from the corals (**C**; $n = 6$), and 7 measurements at various locations along the coral surface (concentration modeled from data that were recorded for ~30 s; **D**; $n = 21$). Superoxide concentrations (mean ± *SD*) were measured in the light during the day (9 am; PAR = ~50 μmol photon m^{-2} s^{-1}; white bars) and in the dark at night (9 pm; PAR = 0 μmol photon m^{-2} s^{-1}; black bars). Note the difference in scale for the y-axes. Significant differences ($p < 0.05$) between day and night superoxide concentrations indicated by an asterisk.

in the combined mucus and tissue samples (89.88 ± 16.68%) compared to just the mucus (30.92 ± 16.16 and 57.47 ± 24.11% mean abundances for days 0 and 4). *Rhodobacteraceae* were also consistent associates of all mucus and combined mucus and tissue samples, with mean abundances ranging from 3.44–4.97%.

Superoxide Production by Representative *Porites* Symbionts

Representative cultures of the most abundant *P. astreoides* symbionts, clade A4 *Symbiodinium* strain CCMP2456 and *E. montiporae* LMG 24815, were examined for their ability to produce extracellular superoxide. Both organisms produced extracellular superoxide in the morning and night in the presence and absence of low light, with steady-state superoxide concentrations ranging from 306.73 ± 59.88 to 795.26 ± 81.55 pM (**Figure 3**; **Table 4**). Although steady state superoxide concentrations were similar between these organisms, cell-normalized rates of superoxide production were consistently several orders of magnitude lower for *E. montiporae* than *Symbiodinium* CCMP2456, with rates ranging from 0.54 ± 0.06 to 1.00 ± 0.29 amol $cell^{-1}$ h^{-1} and 887.8 ± 202.7 to 1353.1 ± 531.5 amol $cell^{-1}$ h^{-1}, respectively. When normalized to cell surface area, superoxide production rates by *Symbiodinium* CCMP2456 (4.22 ± 2.06 to 5.32 ± 2.09 amol μm^{-2} h^{-1}) were still considerably higher than those by *E. montiporae* (0.06 ± 0.01 to 0.11 ± 0.03 amol μm^{-2} h^{-1}; **Table 4**).

In addition to monocultures, extracellular superoxide production was measured in combined samples of *Symbiodinium* CCMP2456 and *E. montiporae*. These were normalized to the total number of *Symbiodinium* CCMP2456 and *E. montiporae* cells and ranged from 0.94 ± 0.14 to 1.24 ± 0.71 amol $cell^{-1}$ h^{-1}. Expected levels of superoxide production by combined cultures were calculated by extrapolating individual superoxide production rates by *Symbiodinium* CCMP2456 and *E. montiporae* under the same temperature conditions

TABLE 3 | Percent composition of major bacterial and archaeal taxa represented in coral colonies (*SD* = standard deviation).

Major taxa	Mucus, Day 0 ($n = 12$)		Mucus, Day 4 ($n = 10$)		Mucus and Tissue ($n = 6$)	
	Range (%)	Mean (%) (*SD*)	Range (%)	Mean (%) (*SD*)	Range (%)	Mean (%) (*SD*)
Bacteroidetes	1.59–5.74	3.16 (1.39)	0.61–5.49	2.57 (1.40)	0.51–6.76	2.22 (2.24)
Synechococcus	0.11–0.52	0.22 (0.15)	0.03–0.38	0.14 (0.11)	0–0.03	0.01 (0.01)
Rhodobacteraceae	1.38–11.21	4.97 (3.00)	1.91–15.92	4.46 (4.10)	0.81–10.43	3.44 (3.61)
SAR11 clade	1.06–5.80	2.16 (1.26)	0.31–0.95	0.59 (0.22)	0.02–0.17	0.10 (0.05)
Sphingomonadales	1.63–7.10	3.95 (1.47)	1.25–6.34	3.72 (1.64)	0.02–0.53	0.14 (0.19)
Rhizobiales	1.47–21.07	13.19 (6.61)	0.61–5.36	2.02 (1.47)	0.17–1.90	0.67 (0.63)
Other Alphaproteobacteria	2.38–7.09	3.45 (1.29)	0.9–8.83	2.86 (2.35)	0.99–4.84	2.06 (1.45)
Endozoicomonas	3.89–55.84	30.92 (16.12)	4.04–84.21	57.47 (24.11)	47.88–93.35	80.88 (16.68)
Alteromonadaceae	1.05–15.42	5.97 (3.96)	0.73–12.16	2.67 (3.40)	0.05–0.95	0.34 (0.32)
Vibrionaceae	0.15–11.82	3.22 (3.22)	0.02–7.34	0.85 (2.28)	0–0.13	0.04 (0.05)
Pseudomonas	0.57–11.39	3.43 (3.48)	0.45–10.07	3.04 (2.73)	n.r.	n.r.
Pseudoalteromonadaceae	0.64–26.67	10.07 (8.61)	0.00–2.25	0.41 (0.67)	n.r.	n.r.
Other Gammaproteobacteria	2.48–13.64	6.08 (3.61)	0.97–8.45	3.04 (2.10)	0.44–4.28	1.47 (1.44)
Oxalobacteraceae	0.30–3.88	1.67 (0.96)	0.50–30.23	11.62 (8.71)	0–0.09	0.03 (0.03)
Other Betaproteobacteria	0.60–5.66	2.87 (1.83)	0.26–3.20	1.64 (0.93)	0.09–1.70	0.42 (0.63)
Other Proteobacteria	0.51–7.27	1.71 (1.82)	0.15–1.76	0.76 (0.58)	0.73–4.42	1.84 (1.43)
Planctomycetes	0.01–0.77	0.39 (0.25)	0.02–1.67	0.42 (0.50)	0.48–9.09	2.66 (3.21)
Other Bacteria	0.81–5.02	2.30 (1.33)	0.43–4.08	1.56 (1.28)	1.48–6.90	3.60 (2.04)
Archaea	0.10–0.47	0.28 (0.12)	0.01–0.53	0.15 (0.15)	0.02–0.16	0.09 (0.06)

n.r. = not represented.
shading key: *Mean 0–5%* *Mean 5–10%* *Mean 10–20%* *Mean >20%*

and at the same time of day. For example, mixed cultures contained approximately 4.4×10^4 and 8.6×10^7 cells of *Symbiodinium* CCMP2456 and *E. montiporae*, respectively, and predicted superoxide production rates for the mixed consortia ranged from 1.10 ± 0.10 to 1.81 ± 0.60 amol cell^{-1} h^{-1} (**Figure 3**). Based on *t*-tests conducted on the difference between measured and calculated production rates under the same light/time conditions, combining the *Symbiodinium* and *E. montiporae* cultures did not have a significant effect on extracellular superoxide production ($p > 0.05$).

The potential effect of low light and time of day on extracellular superoxide production by *Symbiodinium* CCMP2456, *E. montiporae*, and combined cultures were examined. Although the presence of ambient low light levels (PAR = 45–60 μmol photon m^{-2} s^{-1}) generally increased average superoxide production rates by *Symbiodinium* CCMP2456, *E. montiporae*, and combined cultures (**Figure 3**), these increases were not significant ($p > 0.05$) (**Figure 3**; **Table 4**). In fact, the only significant difference was a significant decrease in superoxide production by *E. montiporae* under low light conditions (0.54 ± 0.06 amol cell^{-1} h^{-1}) as opposed to in the dark (0.81 ± 0.04 amol cell^{-1} h^{-1}) during the evening ($p = 0.03$; **Figure 3**).

Other *Symbiodinium* spp. Incubations

To obtain a broader sense of extracellular superoxide production by a variety of *Symbiodinium* strains, we also examined cultures representative of phylogenic clades B2, C1, D, and D1. A wide range of extracellular superoxide production rates was measured for these five *Symbiodinium* strains, from 55.0 ± 2.8 to 1265.4 ± 294.1 amol cell^{-1} h^{-1} (**Figure 4**). The lowest production rates were measured for *Symbiodinium* CCMP3364 (clade B2) and the highest from *Symbiodinium* CCMP2466 and CCMP3408 (clades C1 and D1, respectively) (**Figure 4**). For all cultures, surface-area normalized rates ranged from 0.12 ± 0.01 to 4.17 ± 0.97 amol μm^{-2} h^{-1} (**Table 4**). Due to differences in initial cell densities, these inter-strain comparisons of superoxide production rates must be interpreted with caution, however (see Discussion below).

Extracellular superoxide production rates for each *Symbiodinium* strain were generally higher in the presence of low light than in the dark, but this difference was only statistically significant for *Symbiodinium* CCMP3364 (clade B2), in which the presence of low light stimulated extracellular superoxide production by 50% ($p = 0.04$; **Table 4**). On the other hand, *Symbiodinium* CCMP2466 (clade C1) produced significantly more superoxide in the dark (1183.8 ± 26.1 amol cell^{-1} h^{-1}) than in the presence of low light (830.4 ± 75.4 amol cell^{-1} h^{-1}; $p = 0.03$; **Figure 4**).

DISCUSSION

ROS play a critical yet enigmatic role in coral physiology and health, from bleaching to potential immune defense. Thus,

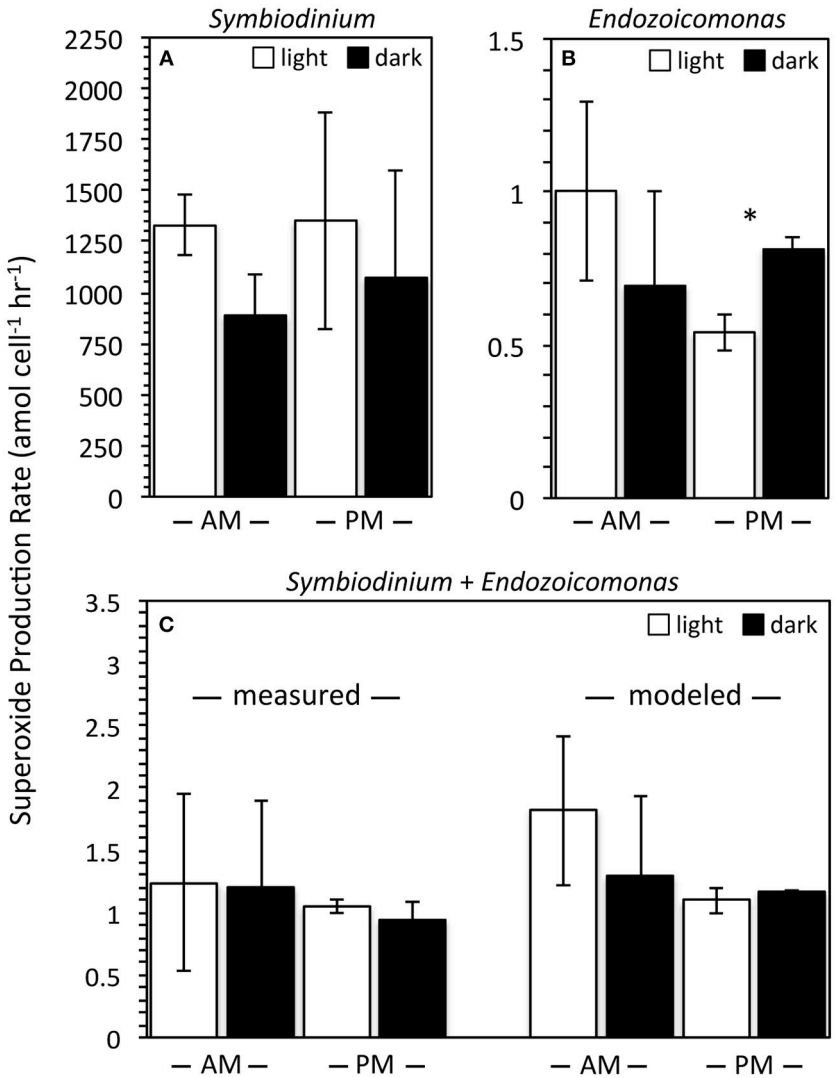

FIGURE 3 | Cell normalized extracellular superoxide production rates (mean ± SEM; $n = 3$) by *Symbiodinium* Clade A4 strain CCMP2456 and *Endozoicomonas montiporae* LMG24815 measured in isolation (A,B) and together **(C)**. Measurements were conducted in the light during the morning (white bars; PAR = ∼50 μmol photon m^{-2} s^{-1}; 9–11 am) and in the dark at night (black bars; PAR = 0 μmol photon m^{-2} s^{-1}; 10–11 pm). *Symbiodinium* + *Endozoicomonas* measurements are normalized to the total number of algal + bacterial cells. Predicted production rates of mixed cultures were calculated by adding individual rates for each organism. Note different scales for the y-axes. Significant differences ($p < 0.05$) between day and night superoxide production rates are indicated by an asterisk.

an improved understanding of the factors that regulate ROS homeostasis in corals is necessary in order to understand the health and functioning of coral reef ecosystems. Here, we examined extracellular superoxide production by aquaria-hosted *P. astreoides* colonies. In these experiments, superoxide was measured in control (coral-free) aquaria, at various background locations within coral-containing aquaria, and at coral surfaces. Background concentrations of superoxide in the experimental and coral-free control aquaria (0.2–1.4 nM; **Figure 2**) were similar to concentrations of superoxide previously observed in productive brackish and marine waters (Rusak et al., 2011; Zhang et al., 2016). Superoxide concentrations at coral surfaces (29.0 ± 7.6 to 41.9 ± 0.9 nM) were 27 to 96 times higher than background seawater concentrations in the same aquarium, which was a significant difference ($p < 0.05$), indicating that corals are a source of superoxide. Consistent with this point source production and with the short lifetime of superoxide in these waters (average half-life in DTPA treated reef water = ∼1.3 min), coral-derived superoxide was limited to the corals' immediate surroundings. For example, within coral-containing aquaria, superoxide concentrations significantly decreased at a distance of only 3 cm from the coral. Superoxide concentrations 3 cm away from the coral surface and at the aquarium surface were similar with the exception of two time

TABLE 4 | Summary of superoxide measurements as the mean ± SEM for biological replicates ($n = 3$) analyzed during mid-exponential growth.

Organism	Cell length (μm)	Cell width (μm)	Cell surface area (μm^2)	Time of day	Light condition	Steady-state concentration (pM)	Production rate (pmol hr^{-1})	Cell normalized* production rate (amol $cell^{-1}$ hr^{-1})	Surface area normalized production rate# (amol μm^{-2} h^{-1})
DIEL EXPERIMENTS									
Symbiodinium CCMP2456 (clade A4)	9	9	254.5[a]	AM	Light	462.92 ± 49.80	55.55 ± 5.98	1328.5 ± 150.11	5.22 ± 0.59
				AM	Dark	314.98 ± 89.08	37.80 ± 10.69	887.81 ± 202.67	3.49 ± 0.80
				PM	Light	408.29 ± 78.15	48.99 ± 9.38	1353.14 ± 531.52	5.32 ± 2.09
				PM	Dark	306.73 ± 59.88	36.81 ± 7.19	1072.59 ± 525.82	4.22 ± 2.07
Endozoicomonas montiporae LMG24815	2	1	9.4[b]	AM	Light	596.75 ± 42.76	71.61 ± 5.13	1.00 ± 0.29	0.11 ± 0.03
				AM	Dark	382.65 ± 70.80	45.92 ± 8.49	0.69 ± 0.31	0.07 ± 0.03
				PM	Light	411.27 ± 59.24	49.35 ± 7.11	0.54 ± 0.06	0.06 ± 0.01
				PM	Dark	615.77 ± 63.48	73.89 ± 7.62	0.81 ± 0.04	0.09 ± 0.00
Symbiodinium CCMP2456 (clade A4) + *E. montiporae* LMG24815			-	AM	Light	633.74 ± 209.67	76.05 ± 25.16	1.24 ± 0.71	–
				AM	Dark	614.87 ± 205.84	73.78 ± 24.70	1.20 ± 0.69	–
				PM	Light	795.26 ± 81.55	95.43 ± 9.79	1.05 ± 0.05	–
				PM	Dark	722.31 ± 154.10	86.68 ± 18.49	0.94 ± 0.14	–
SYMBIODINIUM STRAINS									
Symbiodinium CCMP2456 (clade A4)	9	9	254.5[a]	AM	Light	517.72 ± 90.05	62.13 ± 10.81	740.08 ± 35.38	2.91 ± 0.14
				AM	Dark	349.20 ± 36.15	41.90 ± 4.34	517.70 ± 77.92	2.03 ± 0.31
Symbiodinium CCMP3364 (clade B2)	13.5	11.5	464.4[c]	AM	Light	864.93 ± 74.47	103.79 ± 8.94	84.38 ± 7.26	0.18 ± 0.01
				AM	Dark	564.06 ± 28.69	67.69 ± 3.44	55.03 ± 2.80	0.12 ± 0.01
Symbiodinium CCMP2466 (clade C1)	10	10	314.2[a]	AM	Light	791.01 ± 47.18	94.92 ± 5.66	830.37 ± 75.38	2.64 ± 0.24
				AM	Dark	1139.34 ± 94.33	136.72 ± 11.32	1183.85 ± 26.08	3.77 ± 0.08
Symbiodinium CCMP3408 (clade D1)	10.5	9.5	303.6[c]	AM	Light	861.33 ± 218.12	103.36 ± 26.17	1265.40 ± 294.16	4.17 ± 0.97
				AM	Dark	760.61 ± 118.45	91.27 ± 14.21	1128.17 ± 182.37	3.71 ± 0.60
Symbiodinium CCMP2556 (clade D)#	10	10	314.2[a]	AM	Light	274.39 ± 57.20	32.93 ± 6.86	393.36 ± 165.23	1.25 ± 0.52
				AM	Dark	213.78 ± 53.33	25.65 ± 6.40	310.50 ± 138.30	0.99 ± 0.44

Cell numbers were ~10^5 to 10^6 cells for Symbiodinium spp. and 5×10^7 to 1×10^8 cells for E. montiporae.
#*Surface area calculated as described in methods for [a]sphere, [b]rod, or [c]prolate spheroid.*

points (day 4 and 7 at 9 pm), when superoxide in surface seawater was higher ($p < 0.05$; **Figure 2**). Further, compared to control aquaria that did not contain corals, concentrations of superoxide in seawater at the surface of coral-containing aquaria were typically 52–90% lower. However, this result was only statistically supported ($p < 0.05$) in half the measurements, indicating that the presence of corals did not have a significant influence on superoxide concentrations at the surface of the aquaria. The degradation of coral-derived superoxide is, at least partly, due to the reaction between superoxide and redox active metals, such as iron (Fe) and copper (Cu) (Voelker et al., 2000; Rose, 2012), which were present at relatively high levels in the aquaria seawater (**Table 2**). The higher metal concentrations in control aquaria compared to coral-containing tanks likely reflects direct attenuation and potentially uptake of metals by the corals, because reaction with superoxide would not lead to a decrease in total metal concentrations. Similarly, the decrease in metal concentrations over time in all aquaria, including the coral-free control aquaria, is likely explained by adsorption of the metals to the glass walls of the aquaria.

The superoxide concentrations measured at *P. astreoides* surfaces were not significantly different over the course of the 5-day incubation and thus represent consistent concentrations controlled by simultaneous production and decay reactions at the coral surface (**Figure 2**). In addition, variability in extracellular superoxide production as a function of time of day and presence of low light levels was not observed for *P. astreoides* (**Figure 2**). Although coral colonies produced higher average concentrations of superoxide in the presence of low light in the morning on most days, this trend was not statistically significant ($p > 0.05$), except on day 5 (**Figure 2**). This result may be due to the low light levels used (PAR = ~100 μ mol photon m^{-2} s^{-1}) that may not have been sufficient for significant photosynthetic activity. Nevertheless, this result rules out abiotic photo-oxidation mechanisms as a major source of the superoxide observed, further indicating that the coral itself is producing extracellular superoxide. Moreover, the production

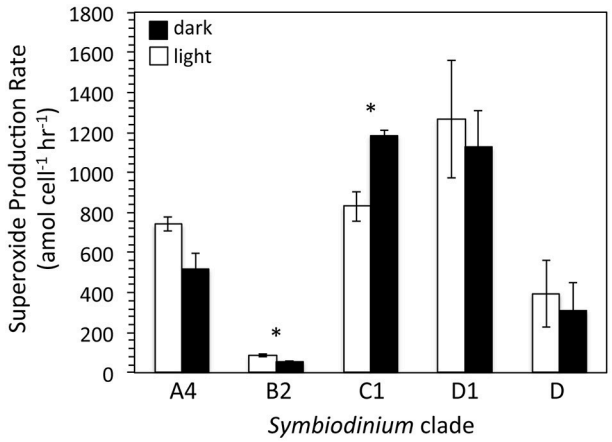

FIGURE 4 | Cell normalized extracellular superoxide production rates (mean ± SEM; $n = 3$, except for clade D $n = 2$) by five different strains of *Symbiodinium*, including CCMP2456 (clade A4), CCMP3364 (clade B2), CCMP2466 (clade C1), CCMP3408 (clade D1), and CCMP2556 (clade D). Measurements were conducted mid-day, either in the light (white bars; PAR = ∼50 μmol photon m^{-2} s^{-1}) and in the dark (black bars; PAR = 0 μmol photon m^{-2} s^{-1}). Significant differences ($p < 0.05$) between day and night superoxide concentrations are indicated by an asterisk.

of extracellular superoxide by *P. astreoides* in the dark indicates that this pathway is independent of photosynthesis. In addition to the results from *P. astreoides* described herein, dark production of both extracellular superoxide and hydrogen peroxide has been shown previously for aquaria-hosted specimens of the coral *Stylophora pistillata* (Saragosti et al., 2010; Armoza-Zvuloni and Shaked, 2014). Thus, non-photosynthetic sources of extracellular ROS clearly exist in multiple coral species.

The superoxide concentrations measured at the surface of *P. astreoides* in this study are among the highest concentrations of superoxide reported for marine systems. For example, coastal and open ocean environments typically exhibit superoxide concentrations in the pM range (Rose, 2012). However, concentrations up to ∼1 nM were previously reported in the surface waters of the Great Barrier Reef (Rose et al., 2010), which is similar to background levels of superoxide in seawater from this study (0.2–1.4 nM). Furthermore, up to ∼33 nM superoxide was reported in association with the deep chlorophyll maximum in one site off the coast of New Zealand, indicating that high biological activity can substantially elevate seawater superoxide concentrations (Rusak et al., 2011). Indeed, in a previous aquaria study, the coral *S. pistillata* increased seawater superoxide concentrations from ∼2 nM (background level) to ∼20 nM in the dark and ∼35 nM in the light (Saragosti et al., 2010), which is similar but slightly lower than the average concentrations reported herein for *P. astreoides* (max 41.9 ± 0.9 nM). Finally, perhaps the highest producer of extracellular superoxide is the ichthyotoxic raphidophyte *Chatonella marina*, which is capable of producing up to 140 nM of superoxide at bloom-level cell densities (Garg et al., 2007). Thus, while the concentrations of *P. astreoides*-derived superoxide are relatively high, they are not entirely unprecedented.

Production of superoxide at the surface of *P. astreoides* may also result in substantial generation of hydrogen peroxide. Hydrogen peroxide concentrations of ∼500 nM have been reported previously at the surface of *Porites* sp. (Shaked and Armoza-Zvuloni, 2013). Whether this hydrogen peroxide derives from direct production at the coral surface, through the reduction of external coral-derived superoxide, and/or through diffusion of internal hydrogen peroxide into the external environment remains unclear. Regardless, external hydrogen peroxide may serve a beneficial role in corals, by acting in prey acquisition and the defense against pathogens regulated by physical and chemical stimuli (Armoza-Zvuloni et al., 2016). Corals also have a strong ability to degrade external hydrogen peroxide (Armoza-Zvuloni and Shaked, 2014) and superoxide (Saragosti et al., 2010), which may presumably be up-regulated if external ROS levels become hazardous to the coral and allow for tight regulation of ROS levels in the coral vicinity.

Superoxide is produced at multiple locations and by different mechanisms within the coral holobiont, including photosynthetic production via the reduction of endogenous O_2 within *Symbiodinium* cells (**Figure 1**). However, as mentioned above (see Introduction), this internal superoxide is unlikely to be detected at coral surfaces. Rather, the most likely sources of external superoxide include epibiotic microbes residing in the coral mucus layer, as well as the coral host's epithelial cells. To test the potential contribution of mucus-associated microbes to external superoxide levels, select *P. astreoides* colonies were dripped to remove the majority of their mucus layer. Mucus-dripped corals produced similar concentrations of superoxide as non-dripped colonies, suggesting that extracellular superoxide fluxes are likely attributable, at least in large part, to the coral host, rather than epibionts. Similarly, previous studies have recognized a prominent role for the coral host in the production of superoxide (Dykens et al., 1992; Nii and Muscatine, 1997; Saragosti et al., 2010) and hydrogen peroxide (Mydlarz and Jacobs, 2006; Shaked and Armoza-Zvuloni, 2013; Armoza-Zvuloni and Shaked, 2014; Armoza-Zvuloni et al., 2016).

Endosymbionts including *Symbiodinium* and tissue-hosted bacteria can be ruled out as contributors to extracellular superoxide observed at the coral surface, but extracellular production by these organisms can contribute to internal (tissue) ROS concentrations, which contribute to internal redox homeostasis and may lead to oxidative stress within the coral host under suboptimal conditions. Similar to previous observations of *Symbiodinium* (CCMP2466, CCMP831) (Saragosti et al., 2010) and heterotrophic bacteria (Learman et al., 2011; Diaz et al., 2013), we observed dark production of extracellular superoxide by non-stressed *Symbiodinium* (CCMP2456, CCMP3364, CCMP2466, CCMP3408, CCMP2556) (**Figure 4**; **Table 4**), as well as non-stressed *E. montiporae* (**Figure 3**; **Table 4**), a widespread and abundant bacterial symbiont of *P. astreoides* and other corals. Significant strain-specific differences in cell-normalized extracellular superoxide production by *Symbiodinium* were observed. However, these results should be interpreted with caution. Cell-normalized extracellular superoxide production has been shown to vary inversely with

cell density (i.e., the number of cells loaded for analysis onto the FeLume) (Marshall et al., 2005; Hansel et al., 2016). Thus, even though production rates are cell-normalized, accurate comparisons between *Symbiodinium* strains can only be made at the same cell density. Because inter-strain comparisons were not the goal of this study, we did not control for the possible effect of cell density between different strains. In other words, the number of cells analyzed was not consistent among the different strains, which prevents our ability to discern whether inter-strain differences were a result of differences in our analytical procedure (i.e., cell load on the FeLume) or actual physiological variability between strains. Consistent with cell density playing a dominant inverse role in extracellular superoxide production, the *Symbiodinium* strain with the lowest superoxide production rate (CCMP3364; Clade B2) was analyzed at a ∼10-fold higher cell density compared to all the other *Symbiodinium* cultures (**Figure 4**). If cell density is inversely related to extracellular superoxide production by *Symbiodinium* in coral tissue, then corals with higher *Symbiodinium* abundances may be less susceptible to superoxide accumulation and oxidative stress, which runs contrary to the previous finding that higher densities of *Symbiodinium* may increase the vulnerability of corals to bleaching (Cunning and Baker, 2013).

Within a single microbial strain (and also for the mixed cultures), identical cell loads were used to generate superoxide measurements in the dark and under low light conditions. Low illumination (PAR = 45–60 μmol photon m^{-2} s^{-1}) did not significantly increase extracellular superoxide production by *E. montiporae* or any *Symbiodinium* strain in our study, with the exception of *Symbiodinium* CCMP3364, in which light enhanced extracellular superoxide production by ∼50% (**Figure 4**). In a previous study that examined extracellular superoxide production by two *Symbiodinium* strains in the presence and absence of heat stress, light significantly stimulated extracellular superoxide production by *Symbiodinium* CCMP2466 (both temperature conditions) and *Symbiodinium* CCMP831 (heat stress only) (Saragosti et al., 2010). However, we also examined *Symbiodinium* CCMP2466 and found the opposite effect: Low illumination significantly attenuated extracellular superoxide production by ∼30% in this organism. This discrepancy is likely due to the low light levels utilized here (45–60 μmol photon m^{-2} s^{-1}) and the higher levels (300 μmol photon m^{-2} s^{-1}) in the previous study (Saragosti et al., 2010). Interestingly, low light levels also significantly decreased extracellular superoxide production by ∼30% in *E. montiporae*, although this only occurred at night and not during the day (**Figure 3**). Overall, our results point to dark pathways of extracellular superoxide production by multiple *Symbiodinium* strains and the coral bacterium *E. montiporae* under non-stressful conditions. Furthermore, extracellular superoxide production by *Symbiodinium* clearly exhibits strain-specific differences in terms of each strain's responsiveness to even low light levels.

In addition to monocultures, we examined extracellular superoxide production by *Symbiodinium* CCMP2456 (clade A4) and *E. montiporae* in the presence of each other under dark and low light conditions at different times of day (**Figure 3**). Although it is unknown whether and to what degree these symbionts may interact within the coral holobiont, our goal was to assess extracellular superoxide production at a level of biological complexity that may be more representative of natural conditions within a coral than microbial monocultures would be. These two organisms did not have an effect on each other, however, both in terms of overall extracellular superoxide production rates and the lack of response of these rates to low light and time of day (**Figure 3**). These results suggest that *Symbiodinium* and *Endozoicomonas* may not interact within corals in any way that would affect internal redox homeostasis.

The lack of day-to-night differences in dark extracellular superoxide production by *P. astreoides* and coral symbionts not only excludes photosynthetic mechanisms of external superoxide generation but also rules out circadian control under these conditions. A variety of physiological processes in corals are thought to be regulated by circadian rhythms, such as calcification, reproduction, and tentacle expansion (for nighttime feeding) (Sorek et al., 2014). A recent study suggests that external release of hydrogen peroxide by *S. pistillata* is associated with zooplankton grazing (Armoza-Zvuloni et al., 2016). However, the day-night uniformity of superoxide concentrations produced by *P. astreoides* here suggests that external superoxide production is not associated with circadian processes such as tentacle expansion and therefore may not play a role in feeding, at least in these corals under the conditions of this study.

Overall, our data indicate that a dark pathway of extracellular superoxide production exists within healthy, pigmented *P. astreoides* and representative coral symbionts, illustrating a lack of dependence of this process on photosynthesis and stress. Therefore, a constant dark pool of superoxide, which is unrelated to stress, is present at the coral surface and within coral tissues, since extracellular superoxide production by non-stressed endosymbionts contributes to internal ROS levels. We speculate that constitutive extracellular sources of dark superoxide may be beneficial to coral health. For example, putative superoxide-generating NADPH oxidases have been implicated in coral thermotolerance (Dixon et al., 2015) and in the resistance of corals to pathogenic white band disease (Libro et al., 2013). Furthermore, superoxide may serve as a defensive mechanism against heat-dependent pathogenic bleaching by the bacterium *Vibrio shiloi*, which expresses an extracellular SOD as a virulence factor (Banin et al., 2003). Extracellular superoxide may also serve a role in coral growth, as proposed for other organisms including bacteria, phytoplankton, and harmful bloom-forming algae, where extracellular superoxide production is a cellular mechanism for controlling cell proliferation (Oda et al., 1995; Saran, 2003; Buetler et al., 2004; Marshall et al., 2005; Hansel et al., 2016).

The findings of this study do not discount photosynthetically-derived ROS production within *Symbiodinium* as an important source of ROS inside coral tissue (Weis, 2008) but instead improve our understanding of ROS homeostasis in corals by supporting a separate pathway of superoxide

generation. Furthermore, our results point to potentially novel aspects of ROS in coral physiology and health, which may have implications for the future of coral reefs. Thus, the physiological role, controls, and consequences of external, dark superoxide production by corals should be investigated further.

AUTHOR CONTRIBUTIONS

CH and AA conceived of the study and designed the experiments. TZ, JD, CB, RP, and SM collected and analyzed the data; JD, CH, and AA interpreted the data and wrote the manuscript with input from TZ, CB, RP, and SM.

FUNDING

This work was supported by a Postdoctoral Fellowship from the Ford Foundation (JD), the National Science Foundation under grants OCE 1225801 (JD) and OCE 1233612 (AA), the Ocean and Climate Change Institute of the Woods Hole Oceanographic Institution (CH), a BIOS Grant in aid award (SM), the Sidney Stern Memorial Trust (CH and AA), as well as an anonymous donor.

ACKNOWLEDGMENTS

Twelve coral colonies and tissue samples were exported from the Bermuda Institute of Ocean Sciences (BIOS) to the Wood Hole Oceanographic Institution under export permits 130801 and 13BM0011 in accordance with the 1972 Bermuda Fisheries Act and the Convention on International Trade in Endangered Species of Wild Fauna and Flora (CITES), respectively, from the Government of Bermuda Department of Conservation Services. We thank Samantha de Putron for assistance with experimental design including the loan of her aquaria, LED lamps and air pumps, Laura Weber for aiding with sample preparation and Chris Wright and the University of Illinois W. M. Keck Center for Comparative and Functional Genomics for sequencing. The authors are grateful to two reviewers whose thoughtful comments greatly improved this manuscript.

REFERENCES

Aguirre, J., Ríos-Momberg, M., Hewitt, D., and Hansberg, W. (2005). Reactive oxygen species and development in microbial eukaryotes. *Trends Microbiol.* 13, 111–118. doi: 10.1016/j.tim.2005.01.007

Andeer, P. F., Learman, D. R., Mcilvin, M., Dunn, J. A., and Hansel, C. M. (2015). Extracellular heme peroxidases mediate Mn(II) oxidation in a marine *Roseobacter* bacterium via superoxide production.. *Environ. Microbiol.* 17, 3925–3936. doi: 10.1111/1462-2920.12893

Apprill, A., Hughen, K., and Mincer, T. (2013). Major similarities in the bacterial communities associated with lesioned and healthy Fungiidae corals. *Environ. Microbiol.* 15, 2063–2072. doi: 10.1111/1462-2920.12107

Apprill, A., Mcnally, S., Parsons, R., and Weber, L. (2015). Minor revision to V4 region SSU rRNA 806R gene primer greatly increases detection of SAR11 bacterioplankton. *Aquat. Microb. Ecol.* 75, 129–137. doi: 10.3354/ame01753

Armoza-Zvuloni, R., Schneider, A., Sher, D., and Shaked, Y. (2016). Rapid hydrogen peroxide release from the coral *Stylophora pistillata* during feeding and in response to chemical and physical stimuli. *Sci. Rep.* 6:21000. doi: 10.1038/srep21000

Armoza-Zvuloni, R., and Shaked, Y. (2014). Release of hydrogen peroxide and antioxidants by the coral *Stylophora pistillata* to its external milieu. *Biogeosciences* 11, 4587–4598. doi: 10.5194/bg-11-4587-2014

Babior, B. M. (1999). NADPH oxidase: an update. *Blood* 93, 1464–1476.

Banin, E., Vassilakos, D., Orr, E., Martinez, R. J., and Rosenberg, E. (2003). Superoxide dismutase is a virulence factor produced by the coral bleaching pathogen *Vibrio shiloi*. *Curr. Microbiol.* 46, 418–422. doi: 10.1007/s00284-002-3912-5

Barott, K. L., Venn, A. A., Perez, S. O., Tambutté, S., and Tresguerres, M. (2015). Coral host cells acidify symbiotic algal microenvironmentsl to promote photosynthesis. *Proc. Nat. Acad. Sci.U.S.A.* 112, 607–612.doi: 10.1073/pnas.1413483112

Bielski, B. H. J., Cabelli, D. E., and Arudi, R. L. (1985). Reactivity of HO_2/O_2^- radicals in aqueous solution. *J. Phys. Chem. Ref. Data* 14, 1041–1100.

Buetler, T. M., Krauskopf, A., and Ruegg, U. T. (2004). Role of superoxide as a signaling molecule. *News Physiol. Sci.* 19, 120–123. doi: 10.1152/nips.01514.2003

Cai, J., and Jones, D. P. (1998). Superoxide in apoptosis. *J. Biol. Chem.* 273, 11401–11404.

Cunning, R., and Baker, A. C. (2013). Excess algal symbionts increase the susceptibility of reef corals to bleaching. *Nat. Clim. Chang.* 3, 259–262. doi: 10.1038/nclimate1711

Diaz, J. M., Hansel, C. M., Voelker, B. M., Mendes, C. M., Andeer, P. F., and Zhang, T. (2013). Widespread production of extracellular superoxide by heterotrophic bacteria. *Science* 340, 1223–1226. doi: 10.1126/science.1237331

Dixon, G. B., Davies, S. W., Aglyamova, G. A., Meyer, E., Bay, L. K., and Matz, M. V. (2015). Genomic determinants of coral heat tolerance across latitudes. *Science* 348, 1460–1462. doi: 10.1126/science.1261224

Dykens, J. A., Shick, J. M., Benoit, C., Buettner, G. R., and Winston, G. W. (1992). Oxygen radical production in the sea anemone *Anthopleura elegantissima* and its symbiotic algae. *J. Exp. Biol.* 168, 219–241.

Edgar, R. C., Haas, B. J., Clemente, J. C., Quince, C., and Knight, R. (2011). UCHIME improves sensitivity and speed of chimera detection. *Bioinformatics* 27, 2194–2200. doi: 10.1093/bioinformatics/btr381

Fujii, M., Rose, A. L., Omura, T., and Waite, T. D. (2010). Effect of Fe(II) and Fe(III) transformation kinetics on iron acquisition by a toxic strain of *Microcytis aeruginosa*. *Environ. Sci. Technol.* 44, 1980–1986. doi: 10.1021/es901315a

Garg, S., Rose, A. L., Godrant, A., and Waite, T. D. (2007). Iron uptake by the ichthyotoxic *Chattonella marina* (raphidophyceae): impact of superoxide generation. *J. Phycol.* 43, 978–991. doi: 10.1111/j.1529-8817.2007.00394.x

Giovannoni, S. J., Delong, E. F., Schmidt, T. M., and Pace, N. R. (1990). Tangential flow filtration and preliminary phylogenetic analysis of marine picoplankton. *Appl. Environ. Microbiol.* 56, 2572–2575.

Giovannoni, S. J., Rappé, M. S., Vergin, K., and Adair, N. (1996). 16S rRNA genes reveal stratified open ocean bacterioplankton popoulations related to the green non-sulfur bacteria phylum. *Proc. Natl. Acad. Sci. U.S.A.* 93, 7979–7984.

Green, D. H., Edmunds, P. J., and Carpenter, R. C. (2008). Increasing relative abundance of *Porites astreoides* on Caribbean reefs mediated by an overall decline in coral cover. *Mar. Ecol. Prog. Ser.* 359, 1–10. doi: 10.3354/meps07454

Guillard, R. R. L., and Hargraves, P. E. (1993). *Stichochrysis immobilis* is a diatom, not a chrysophyte. *Phycologia* 32, 234–236.

Hansard, S. P., Vermilyea, A. W., and Voelker, B. M. (2010). Measurements of superoxide radical concentration and decay kinetics in the Gulf of Alaska. *Deep Sea Res. Part I Oceanogr. Res. Pap.* 57, 1111–1119. doi: 10.1016/j.dsr.2010.05.007

Hansel, C. M., Buchwald, C., Diaz, J. M., Ossolinski, J. E., Dyhrman, S. T., Van Mooy, B. A. S., et al. (2016). Dynamics of extracellular superoxide production by *Trichodesmium* colonies from the Sargasso Sea. *Limnol. Oceanogr.* 61, 1188–1200. doi: 10.1002/lno.10266

Heller, M. I., and Croot, P. L. (2010). Application of a superoxide (O_2^-) thermal source (SOTS–1) for the determination and calibration of O_2^- fluxes in seawater. *Anal. Chim. Acta* 667, 1–13. doi: 10.1016/j.aca.2010.03.054

Jones, R. J., Hoegh-Guldberg, O., Larkum, A. W. D., and Schreiber, U. (1998). Temperature-induced bleaching of corals begins with impairment of the CO_2 fixation mechanism in zooxanthellae. *Plant Cell Environ.* 21, 1219–1230.

Korshunov, S. S., and Imlay, J. A. (2002). A potential role for periplasmic superoxide dismutase in blocking the penetration of external superoxide into the cytosol of Gram-negative bacteria. *Mol. Microbiol.* 43, 95–106. doi: 10.1046/j.1365-2958.2002.02719.x

Kozich, J. J., Westcott, S. L., Baxter, N. T., Highlander, S., and Schloss, P. D. (2013). Development of a dual-index sequencing strategy and curation pipeline for analyzing amplicon sequence data on the MiSeq Illumina sequencing platform. *Appl. Environ. Microbiol.* 79, 5112–5120. doi: 10.1128/AEM.01043-13

Kustka, A. B., Shaked, Y., Milligan, A. J., King, D. W., and Morel, F. M. M. (2005). Extracellular production of superoxide by marine diatoms: Contrasting effects on iron redox chemistry and bioavailability. *Limnol. Oceanogr.* 50, 1172–1180. doi: 10.4319/lo.2005.50.4.1172

Learman, D. R., Voelker, B. M., Vazquez-Rodriguez, A. I., and Hansel, C. M. (2011). Formation of manganese oxides by bacterially generated superoxide. *Nature Geosci.* 4, 95–98. doi: 10.1038/ngeo1055

Lesser, M. P. (2006). Oxidative stress in marine environments: Biochemistry and physiological ecology. *Annu. Rev. Physiol.* 68, 253–278. doi: 10.1146/annurev.physiol.68.040104.110001

Lesser, M. P. (2011). "Coral bleaching: causes and mechanisms," in *Coral Reefs: An Ecosystem in Transition,* eds Z. Dubinsky and N. Stambler (Dordrecht: Springer Netherlands), 405–419.

Libro, S., Kaluziak, S. T., and Vollmer, S. V. (2013). RNA-seq profiles of immune related genes in the staghorn coral *Acropora cervicornis* infected with white band disease. *PLoS ONE* 8:e81821. doi: 10.1371/journal.pone.0081821

Lichtenberg, M., Larkum, A. W., and Kuhl, M. (2016). Photosynthetic acclimation of Symbiodinium in hospite depends on vertical position in the tissue of the scleractinian coral *Montastrea curta*. *Front. Microbiol.* 7:230. doi: 10.3389/fmicb.2016.00230

Marshall, J.-A., Ross, T., Pyecroft, S., and Hallegraeff, G. (2005). Superoxide production by marine microalgae II. Towards understanding ecological consequences and possible functions. *Mar. Biol.* 147, 541–549. doi: 10.1007/s00227-005-1597-6

Mass, T., Einbinder, S., Brokovich, E., Shashar, N., Vago, R., Erez, J., et al. (2007). Photoacclimation of *Stylophora pistillata* to light extremes: metabolism and calcification. *Mar. Ecol. Prog. Ser.* 334, 93–102. doi: 10.3354/meps334093

Minibayeva, F., Kolesnikov, O., Chasov, A., Beckett, R. P., Lüthje, S., Vylegzhanina, N., et al. (2009). Wound-induced apoplastic peroxidase activities: their roles in the production and detoxification of reactive oxygen species. *Plant Cell Environ.* 32, 497–508. doi: 10.1111/j.1365-3040.2009.01944.x

Morrow, K. M., Moss, A. G., Chadwick, N. E., and Liles, M. R. (2012). Bacterial associates of two Caribbean coral species reveal species-specific distribution and geographic variability. *Appl. Environ. Microbiol.* 78, 6438–6449. doi: 10.1128/AEM.01162-12

Mydlarz, L. D., and Jacobs, R. S. (2006). An inducible release of reactive oxygen radicals in four species of gorgonian corals. *Mar. Freshw. Behav. Physiol.* 39, 143–152. doi: 10.1080/10236240600708512

Nii, C. M., and Muscatine, L. (1997). Oxidative stress in the symbiotic sea anemone *Aiptasia pulchella* (Carlgren, 1943): Contribution of the animal to superoxide ion production at elevated temperature. *Biol. Bull.* 192, 444–456. doi: 10.2307/1542753

Oda, T., Moritomi, J., Kawano, I., Hamaguchi, S., Ishimatsu, A., and Muramatsu, T. (1995). Catalase-induced and superoxide dismutase-induced morphological changes and growth inhibition in the red tide phytoplankton *Chattonella marina*. *Biosci. Biotechnol. Biochem.* 59, 2044–2048.

Pandolfi, J. M., and Jackson, J. B. (2006). Ecological persistence interrupted in Caribbean coral reefs. *Ecol. Lett.* 9, 818–826. doi: 10.1111/j.1461-0248.2006.00933.x

Pochon, X., Putnam, H. M., Burki, F., and Gates, R. D. (2012). Identifying and characterizing alternative molecular markers for the symbiotic and free-living dinoflagellate genus *Symbiodinium*. *PLoS ONE* 7:e29816. doi: 10.1371/journal.pone.0029816

Porter, K. G., and Feig, Y. S. (1980). The use of DAPI for identifying and counting aquatic microflora. *Limnol. Oceanogr.* 25, 943–948.

Rodriguez-Lanetty, M., Granados-Cifuentes, C., Barberan, A., Bellantuono, A. J., and Bastidas, C. (2013). Ecological inferences from a deep screening of the complex bacterial consortia associated with the coral, *Porites astreoides*. *Mol. Ecol.* 22, 4349–4362. doi: 10.1111/mec.12392

Roe, K. L., and Barbeau, K. A. (2014). Uptake mechanisms for inorganic iron and ferric citrate in *Trichodesmium erythraeum* IMS101. *Metallomics* 6, 2042–2051. doi: 10.1039/c4mt00026a

Roe, K. L., Schneider, R. J., Hansel, C. M., and Voelker, B. M. (2016). Measurement of dark, particle-generated superoxide and hydrogen peroxide production and decay in the subtropical and temperate North Pacific Ocean. *Deep Sea Res. Part I Oceanogr. Res. Pap.* 107, 59–69. doi: 10.1016/j.dsr.2015.10.012

Rohwer, F., Seguritan, V., Azam, F., and Knowlton, N. (2002). Diversity and distribution of coral-associated bacteria. *Mar. Ecol. Prog. Ser.* 243, 1–10. doi: 10.3354/meps243001

Rose, A. L. (2012). The influence of extracellular superoxide on iron redox chemistry and bioavailability to aquatic microorganisms. *Front. Microbiol.* 3:124. doi: 10.3389/fmicb.2012.00124

Rose, A. L., Godrant, A., Furnas, M., and Waite, T. D. (2010). Dynamics of nonphotochemical superoxide production and decay in the Great Barrier Reef lagoon. *Limnol. Oceanogr.* 55, 1521–1536. doi: 10.4319/lo.2010.55.4.1521

Rose, A. L., Moffett, J. W., and Waite, T. D. (2008a). Determination of superoxide in seawater using 2-methyl-6-(4-methoxyphenyl)-3,7-dihydroimidazo[1,2-a]pyrazin-3(7*H*)-one chemiluminescence. *Anal. Chem.* 80, 1215–1227. doi: 10.1021/ac7018975

Rose, A. L., Salmon, T. P., Lukondeh, T., Neilan, B. A., and Waite, T. D. (2005). Use of superoxide as an electron shuttle for iron acquisition by the marine cyanobacterium *Lyngbya majuscula*. *Environ. Sci. Technol.* 39, 3708–3715. doi: 10.1021/es048766c

Rose, A. L., Webb, E. A., Waite, T. D., and Moffett, J. W. (2008b). Measurement and implications of nonphotochemically generated superoxide in the equatorial Pacific Ocean. *Environ. Sci. Technol.* 42, 2387–2393. doi: 10.1021/es7024609

Rusak, S. A., Peake, B. M., Richard, L. E., Nodder, S. D., and Cooper, W. J. (2011). Distributions of hydrogen peroxide and superoxide in seawater east of New Zealand. *Mar. Chem.* 127, 155–169. doi: 10.1016/j.marchem.2011.08.005

Saragosti, E., Tchernov, D., Katsir, A., and Shaked, Y. (2010). Extracellular production and degradation of superoxide in the coral *Stylophora pistillata* and cultured *Symbiodinium*. *PLoS ONE* 5:e12508. doi: 10.1371/journal.pone.0012508

Saran, M. (2003). To what end does nature produce superoxide? NADPH oxidase as an autocrine modifier of membrane phospholipids generating paracrine lipid messengers. *Free Radic. Res.* 37, 1045–1059. doi: 10.1080/10715760310001594631

Savage, A. M., Trapido-Rosenthal, H., and Douglas, A. E. (2002). On the functional significance of molecular variation in *Symbiodinium*, the symbiotic algae of Cnidaria: photosynthetic response to irradiance. *Mar. Ecol. Prog. Ser.* 244, 27–37. doi: 10.3354/meps244027

Schloss, P. D., Westcott, S. L., Ryabin, T., Hall, J. R., Hartmann, M., Hollister, E. B., et al. (2009). Introducing mothur: open-source, platform-independent, community-supported software for describing and comparing microbial communities. *Appl. Environ. Microbiol.* 75, 7537–7541. doi: 10.1128/AEM.01541-09

Shaked, Y., and Armoza-Zvuloni, R. (2013). Dynamics of hydrogen peroxide in a coral reef: Sources and sinks. *J. Geophys. Res. Biogeosci.* 118, 1793–1801. doi: 10.1002/2013jg002483

Sorek, M., Díaz-Almeyda, E. M., Medina, M., and Levy, O. (2014). Circadian clocks in symbiotic corals: The duet between *Symbiodinium* algae and their coral host. *Mar. Genomics* 14, 47–57. doi: 10.1016/j.margen.2014.01.003

Tchernov, D., Gorbunov, M. Y., de Vargas, C., Narayan Yadav, S. N., Milligan, A. J., Häggblom, M., et al. (2004). Membrane lipids of symbiotic algae are diagnostic of sensitivity to thermal bleaching in corals. *Proc. Nat. Acad. Sci. U.S.A.* 101, 13531–13535. doi: 10.1073/pnas.0402907101

Van Waasbergen, L. G., Hoch, J. A., and Tebo, B. M. (1993). Genetic analysis of manganese oxidation in the marine *Bacillus* sp. strain SG-1: Tn917 mutagenesis and identification of two major loci involved in manganese oxidation. *J. Bacteriol.* 175, 7594–7603. doi: 10.1128/AEM.68.2.874-880.2002

Venn, A. A., Loram, J. E., and Douglas, A. E. (2008). Photosynthetic symbiosis in animals. *J. Exp. Biol.* 59, 1069–1080. doi: 10.1093/jxb/erm328

Venn, A. A., Tambutté, E., Lotto, S., Zoccola, D., Allemand, D., and Tambutté, S. (2009). Imaging intracellular pH in a reef coral and symbiotic anemone. *Proc. Nat. Acad. Sci.* 106, 16574–16579. doi: 10.1073/pnas.0902894106

Voelker, B. M., Sedlak, D. L., and Zafiriou, O. C. (2000). Chemistry of superoxide radical in seawater: reactions with organic Cu complexes. *Environ. Sci. Technol.* 34, 1036–1042. doi: 10.1021/es990545x

Weinberger, F. (2007). Pathogen-induced defense and innate immunity in macroalgae. *Biol. Bull.* 213, 290–302. doi: 10.2307/25066646

Weis, V. M. (2008). Cellular mechanisms of Cnidarian bleaching: stress causes the collapse of symbiosis. *J. Exp. Biol.* 211, 3059–3066. doi: 10.1242/jeb.009597

Yang, C.-S., Chen, M.-H., Arun, A. B., Chen, C. A., Wang, J.-T., and Chen, W.-M. (2010). *Endozoicomonas montiporae* sp. nov., isolated from the encrusting pore coral *Montipora aequituberculata*. *International J. Syst. Evol. Microbiol.* 60, 1158–1162. doi: 10.1099/ijs.0.014357-0

Zhang, T., Hansel, C. M., Voelker, B. M., and Lamborg, C. H. (2016). Extensive dark biological production of reactive oxygen species in brackish and freshwater ponds. *Environ. Sci. Technol.* 50, 2983–2993. doi: 10.1021/acs.est.5b03906

Zhang, Z., Green, B. R., and Cavalier-Smith, T. (2000). Phylogeny of ultra-rapidly evolving dinoflagellate chloroplast genes: a possible common origin for sporozoan and dinoflagellate plastids. *J. Mol. Evol.* 51, 26–40. doi: 10.1007/s002390010064

Conflict of Interest Statement: The authors declare that the research was conducted in the absence of any commercial or financial relationships that could be construed as a potential conflict of interest.